JOURNAL OF GEOPHYSICAL RESEARCH, VOL. 95, NO. D9, PAGES 13,749–13,764, AUGUST 20, 1990

The Dependence of Constituent Transport on Chemistry in a Two-Dimensional Model of the Middle Atmosphere

ANNE K. SMITH

Space Physics Research Laboratory, Department of Atmospheric, Oceanic and Space Science University of Michigan, Ann Arbor

GUY P. BRASSEUR

National Center for Atmospheric Research, Boulder, Colorado

The transport of trace species by waves is affected by their production and/or destruction by photochemical processes. For this reason the transport or "diffusion" matrices used in two-dimensional models should be different for each constituent. This paper describes a method for altering the meridional and vertical dynamical transport coefficients for use with photochemically active species. The transport represents the net meridional eddy flux by planetary waves and the net vertical eddy flux by gravity waves. Output from integrations using the control (species independent) and chemical eddy transport coefficients are compared. The change in the meridional (planetary wave) transport results in modest, but nevertheless significant, changes in the distribution of trace species. In many cases, for example odd oxygen and nitric acid, the model changes bring the distributions closer to those observed. In contrast, the incorporation of the chemical eddy effect into the gravity wave transport has almost no effect on any of the model fields.

1. Introduction

The chemical, dynamical, radiative interactions in the middle atmosphere are sufficiently complex that comprehensive three dimensional models are still not available. Three-dimensional studies of the stratospheric chemistry and dynamics [*Mahlman and Moxim*, 1978; *Grose et al.*, 1987; *Kaye and Rood*, 1989; *Rose and Brasseur*, 1989] decouple chemistry from dynamics, use simplified chemistry and are limited to short integrations (one week to one season). In the mesosphere, where small scale waves play a dominant role in driving the circulation, a global three-dimensional (3D) simulation of even the dynamics alone is out of the range of all except the highest resolution models [*Mahlman and Umsheid*, 1987]. For simulations of long time scales (one or more years), zonally averaged two-dimensional (2D) models are the best tools presently available. Numerous studies have used 2D models to study the middle atmosphere chemistry and dynamics [*Garcia and Solomon*, 1983, 1985; *Guthrie et al.*, 1984; *Jones and Pyle*, 1984; *Ko et al.*, 1985; *Stordal et al.*, 1985; *Pitari and Visconti*, 1985; *Brasseur et al.*, 1990]. For these models, zonal perturbations, such as those due to Rossby, tropical and gravity waves, are not explicitly modeled but their effect on the mean fields must be determined in some way (or omitted, as has been the case for tropical waves).

Interaction of breaking or dissipating gravity waves with the mean flow is important in driving of the mean circulation in the mesosphere through vertical momentum flux divergence. In addition, the turbulence associated with breaking waves results in vertical transport of heat and chemical constituents. These have been parameterized by Rayleigh friction [*Wehrbein and Leovy*, 1982] with a prescribed vertical diffusion coefficient for eddy transport of chemical species [*Garcia and Solomon*, 1983]. Also several models [*Holton and Schoeberl*, 1988; *Garcia and Solomon*, 1985; *Brasseur and Hitchman*, 1987] use adaptations of the breaking gravity wave parameterization introduced by *Lindzen* [1981]. The Lindzen parameterization, although conceptually and computationally simple, allows the impact of gravity waves to vary as the mean flow varies and hence includes a degree of feedback. The vertical diffusion coefficient varies with season due to the modulation of gravity wave propagation by the winds in the middle atmosphere. Observations of gravity wave interactions are sparse, so in practice the details of the parameterization are guided by the need to reproduce the observed structure of temperature and of a few trace species for which observations of seasonal variations and vertical structure are available.

Rossby waves also act to drive the mean flow and to transport chemical constituents both vertically and horizontally. The treatment in two-dimensional models ranges from prescribing the diabatic heating rate and horizontal diffusion [*Guthrie et al.*, 1984; *Stordal et al.*, 1985] to a quasi-3D treatment coupling a wave model that computes wave transports directly [*Pyle and Rogers*, 1980]. Several approaches have been used to insure that the model mean flow is consistent with the eddy transport. *Pitari and Visconti* [1985] and *Plumb and Mahlman* [1987] used both the eddy transport and mean circulation derived from fields generated by the same 3D model; *Tung* [1987] specified the mean temperature field and derived the eddy transport needed to maintain it; and *Hitchman and Brasseur* [1988] parameterized the eddy transport based on the 2D structure of the model mean flow.

An issue that has been considered in several studies is the effect of variations in the eddy diffusion, particularly the meridional diffusion coefficient K_{yy}, on the distribution of trace species in 2D models. *Guthrie et al.* [1984], *Ko et al.* [1985], and *Stordal et al.* [1985] all used a diabatic circulation based on observations and assessed the effect of variations in K_{yy} on the distribution of one or more trace species. The effect

Paper number 90JD00445.
0148-0227/90/90JD-00445$05.00

of eddies in driving the mean circulation was not explicitly calculated in these models. This omission can result in an unrealistic conclusion about the sensitivity of the chemical distribution to K_{yy}. This was made evident in a recent study by *Schneider et al.* [1989]. They found that the sensitivity of the ozone distribution to the parameterized eddy diffusion results from two effects that can cancel one another. The eddy diffusion of ozone, which can have a large impact on the zonally averaged distribution, results from the presence of eddies in the dynamical fields, notably potential vorticity (pv). The eddy transport of pv is a main component to the driving of the mean meridional circulation. Increased K_{yy} in the ozone continuity equation tends to flatten the ozone gradient, but that same increase, when applied to pv transport, can lead to a stronger mean circulation. The increase in mean advection has the effect of steepening the meridional ozone gradient, and can therefore offset the gradient weakening effect of increased diffusion. Schneider et al used a single, spatially uniform, diffusion coefficient for the transport of pv, which gives mean flow driving, and for ozone.

In all of the models mentioned here, the transport of trace species is represented, at least in part, by an eddy transport matrix **K** multiplied by the mean gradient of the tracer mixing ratio, although in some cases **K** is limited to its diagonal components (K_{yy} and/or K_{zz}). This simple flux gradient relationship can be inadequate if the photochemical damping rate of the trace species has an eddy component due to variations in chemical loss rate with temperature or with the distribution of other species. Additional contributions to the net flux resulting from temperature dependence and coupled chemistry were included in two dimensional models of *Garcia and Solomon* [1983] and *Pitari and Visconti* [1985], respectively. The primary effect of Rossby waves is meridional transport, so K_{yy} is chosen to represent this; in models in which K_{yy} varies spatially, it is largest in the winter stratosphere and subtropics. Gravity wave breaking and the associated turbulence are assumed to contribute primarily to vertical mixing, so K_{zz} is normally largest in the mesosphere.

A number of studies have shown that **K** should vary with species for photochemically active tracers [*Pyle and Rogers*, 1980; *Matsuno*, 1980; *Garcia and Solomon*, 1983; *Smith et al.*, 1988]. This is due to the contribution to transport from the "chemical eddy" effect, resulting from variations in the production and loss rates as air flows through the wave. The effect is largest in that region between the domain of dynamical control (slow chemistry) and chemical control (rapid chemistry), known as the transition region [*Hartmann and Garcia*, 1979]. There the dynamical time scale, defined as the time it takes an air parcel to flow through the wave, is comparable to the time scale for photochemical production and loss. The contribution of the chemical eddy effect to the net eddy transport is not as strong in regions where either transport or photochemistry strongly dominates in controlling the trace species distribution.

In this paper, the impact of the chemical eddy effect on parameterized meridional and vertical transport for photochemically active species and families in the middle atmosphere is calculated. The study uses the 2D model described by *Brasseur et al.* [1990]. Chemical eddy transport coefficients and contributions to transport from the temperature dependence of the photochemical loss rate are determined for Rossby waves and gravity waves. For this study the parameterizations of *Lindzen* [1981] and *Hitchman and Brasseur* [1988] are used.

2. Rossby Wave Chemical Eddy Transport

2.1. *Transport Matrix for a Nonconserved Trace Species*

The general form used for eddy transport is

$$\overline{v'\mu'} = -\mathbf{K}\cdot\nabla\bar{\mu} \tag{1}$$

where μ represents the mixing ratio of tracer and the four components of **K** are identified as

$$\mathbf{K}=\begin{pmatrix} K_{yy} & K_{yz} \\ K_{zy} & K_{zz} \end{pmatrix}$$

A number of derivations, basically similar but using different assumptions, have been used for determining the matrix **K** from the eddy continuity equation for a trace species [*Plumb*, 1979; *Matsuno*, 1980; *Holton*, 1981; *Pyle and Rogers*, 1980; *Strobel*, 1981; *Tung*, 1982; *Garcia and Solomon*, 1983; *Smith et al.*, 1988]. In all cases, the approximation of small amplitude is used to derive **K**, although **K** can be determined empirically without such an assumption [*Newman et al.*, 1986; 1988; *Plumb and Mahlman*, 1987]. The derivation of **K** will not be repeated here. A fairly general form is that given by *Strobel* [1981], which includes the effects of linear photochemical damping, temperature dependence of the photochemistry, wave transience, traveling waves, and damping of temperature by Newtonian cooling.

With temperature dependent photochemistry, the eddy transport is no longer given by the simple flux/gradient relation (1), but acquires an additional contribution that can be expressed as a matrix $\mathbf{K}^T$ multiplied by the mean gradient of potential temperature [*Garcia and Solomon*, 1983; *Smith et al.*, 1988]

$$\overline{v'\mu'} = -\mathbf{K}\cdot\nabla\bar{\mu} + \mathbf{K}^T\cdot(T/\theta\nabla\bar{\theta}) \tag{2}$$

or as a matrix $\mathbf{K}_2$ multiplied by the mean tracer mixing ratio [*Strobel*, 1981]

$$\overline{v'\mu'} = -\mathbf{K}\cdot\nabla\bar{\mu} + \mathbf{K}_2\cdot\bar{\mu} \tag{3}$$

In writing the temperature dependence in the form (2), we have expressed eddy quantities in terms of eddy displacements (η', ζ'), defined as

$$(v',w') = \frac{d}{dt}(\eta',\zeta') \tag{4}$$

rather than in terms of v', T', etc. This allows all eddy quantities in **K** and $\mathbf{K}^T$ to be written in terms of four displacement correlations, $\overline{\eta'^2}$, $\overline{\zeta'^2}$, $\overline{\eta'\zeta'}$, and $\overline{i\eta'\zeta'}$ [*Garcia and Solomon*, 1983; *Smith et al.*, 1988].

For Rossby waves, the largest contribution to the transport comes from the K_{yy} $(\partial\bar{\mu}/\partial y)$ term, although K_{yz} $(\partial\bar{\mu}/\partial z)$ can also be significant for a trace species that is strongly vertically stratified [*Smith et al.*, 1988]. In our model we do not use the full matrix **K** but only the diagonal terms K_{yy} and K_{zz}, determined from the Rossby and gravity wave parameterizations respectively.

2.2. *Eddy Transport Due to Rossby Waves in the 2D model*

The Rossby wave parameterization derived by *Hitchman and Brasseur* [1988] is based on the WKB assumption that the direction of wave propagation is determined by the structure of the mean flow. This can be quantified as a conservation equation for wave activity

$$\frac{\partial A}{\partial t} + \nabla \cdot \mathbf{c}_g A = -\alpha A \tag{5}$$

Wave activity is specified at the tropopause, is advected by the Rossby wave group velocity $\mathbf{c}_g$, and is absorbed by wave damping ($-\alpha A$). The group velocity is determined from the mean flow structure. A wave activity forcing that varies with latitude and season is applied at the tropopause and a height-dependent damping rate is assumed. In the WKB approximation, the EP flux divergence, used to determine the mean flow forcing by the dissipating Rossby wave, is given by $\nabla \cdot \mathbf{F} = \nabla \cdot \mathbf{c}_g A$. The meridional eddy transport coefficient is obtained by noting that $\nabla \cdot F$ is proportional to $\overline{v'q'}$, where q is quasi-geostrophic potential vorticity [*Edmon et al.*, 1980]. Defining the transport coefficient from the flux gradient relation gives $K_{yy} = -\overline{v'q'} / (\partial \bar{q}/\partial y)$. The mean pv gradient $\partial \bar{q}/\partial y$ is a function of the mean zonal wind, and is therefore known.

In the present study a modification was made to the Hitchman and Brasseur parameterization to account for the enhanced transport that occurs in the region known as the surf zone [*McIntyre and Palmer*, 1983] that is normally located in or near the subtropics of the winter/spring hemisphere. The modification increases the damping rate of wave activity wherever the zonal mean potential vorticity gradient disappears or becomes negative. The effect of this is an enhancement of K_{yy} in the subtropics and a decrease in that extending across the equator into the summer hemisphere.

In order to relate the eddy transport for an arbitrary tracer to that for pv, we first need to understand what physical mechanisms are responsible for pv transport, and how they combine to give the transport coefficient K_{yy}. The eddy flux of constituents results from transience and from dissipation [*Charney and Drazin*, 1961], which are contained in the first term on the left-hand side and in the right-hand side of (5), respectively. Also, if a limited wave number range or horizontal resolution is considered, wave-wave interactions can give a net transport of pv within that range. Transience alone will not have any net effect when averaged over long times, but when accompanied by mean flow variations or damping of any kind, it does not average to zero [*Andrews and McIntyre*, 1976]. The dissipation of pv is assumed to be due to two processes: radiative damping of waves and effective damping because of interaction of the waves with smaller horizontal scales and loss of pv at those smaller scales. When comparing pv transport to transport of a trace species, it is necessary to separate those dissipation processes that act only on pv, such as radiative damping, from dynamical processes that affect any field that is not uniformly distributed. Although pv transport can be compared with that of a trace chemical species, as if both were tracers, it is also useful to remember that whenever there is any meridional eddy transport ($v' \neq 0$), then pv perturbations, although not necessarily pv transport, must be nonzero [*Hoskins et al.*, 1985]. The dual nature of the pv transport, resulting both from dissipation of pv and from unresolved dynamical interactions, introduces a complication into the present calculations since the *Hitchman and Brasseur* [1988] parameterization applies a single damping rate to account for all effects. In essence, they have assumed that the net effect over long periods of nonlinearity or short-term transience can be expressed as a linear damping that can be added to the effect of damping of pv. α represents the total effect of all "damping" processes.

The other complication in using the *Hitchman and Brasseur* [1988] parameterization for chemical eddy calculations is that quasi-geostrophic pv is, by definition, transported only horizontally. This means that only the K_{yy} component of $\mathbf{K}$ is needed for pv. Additional assumptions about wave structure would be needed to determine the three other components of $\mathbf{K}$ due to Rossby waves.

2.3. *Calculation of the Chemical Eddy Transport*

To determine how the meridional eddy transport coefficient for any given species is related to that for pv, we begin with a general expression for K_{yy} for a nonconserved quantity. The wave form assumed is $\mu' \sim \exp[i(kx+\sigma t)]$, where σ can have real and imaginary parts, representing traveling and growing or decaying waves, respectively. The linearized eddy continuity equation is

$$\left(\frac{\partial}{\partial t} + \bar{u}\frac{\partial}{\partial x}\right)\mu' + v'\frac{\partial \bar{\mu}}{\partial y} + w'\frac{\partial \bar{\mu}}{\partial z} = -\bar{L}\mu' - \overline{GT}'\bar{\mu} \tag{6}$$

where L represents the photochemical loss rate and $G = d\bar{L}/dT$. In writing (6), we have made the approximation that the loss rate varies in the zonal direction only due to its dependence on temperature and not, for example, because of the diurnal cycle or because of perturbations in the mixing ratios of other trace species with which it interacts. In addition to all eddy products, advection by the mean meridional circulation and production/loss of μ' that cannot be expressed as a linear relaxation back to a mean distribution are neglected. The real part of the wave frequency for Rossby waves is neglected; the imaginary part, i.e. that due to wave growth and decay, is denoted by σ_i. Combining (6) and the flux-gradient relation (1), and neglecting temperature dependence of the photochemistry (i.e., $\bar{G} = 0$), with $\mathbf{K}$ reduced to a single coefficient K_{yy}, it is straightforward to obtain an expression for K_{yy}.

$$K_{yy} = \frac{L+\sigma_i}{\left(k\bar{u}\right)^2 + (L+\sigma_i)^2}\left[\left(k\bar{u}\right)^2 + (\sigma_i)^2\right]\overline{\eta'^2} \tag{7}$$

It is evident from (7) that there is no transport unless either photochemical damping L or transience σ_i is nonzero. K_{yy} is linearly proportional to $L+\sigma_i$ when the chemical loss rate is small ($L \ll \sigma_i$) and K_{yy} is inversely proportional to L when it is large ($L \gg \sigma_i, k\bar{u}$). For a photochemical loss time scale that is comparable in magnitude to the dynamical time scale, it is not possible to separate $\mathbf{K}$ into two matrices representing dispersion and chemical eddy transport, as was done by *Plumb* [1979] for weak photochemistry. It is evident from (7) that the the effect of transience is added to L so, in effect, wave transience acts much like an additional damping term that is the same for all species. The form of K_{yy} given in (7) follows from the assumptions made in the derivation (linearity, production and loss limited to linear damping) and is limited by those same assumptions.

For a species μ, with photochemical damping rate L_μ, K_{yy} will be related to that of pv (denoted by q, with damping rate L_q) by

$$(K^\mu)_{yy} = \left[\frac{L_\mu + \sigma_i}{L_q + \sigma_i}\right] \cdot \left[\frac{(k\bar{u})^2 + (L_q + \sigma_i)^2}{(k\bar{u})^2 + (L_\mu + \sigma_i)^2}\right] \cdot (K^q)_{yy} \qquad (8)$$

The contribution to meridional transport $\overline{v'\mu'}$ from temperature dependence of chemical reaction rates is $(K^T)_{yy}$ $(\partial\bar{T}/\partial y) + (K^T)_{yz}$ $(\bar{T}/\bar{\theta})$ $\partial\bar{\theta}/\partial z$, where

$$(K^T)_{yy} = \frac{G\bar{\mu}}{(k\bar{u})^2 + (L+\sigma_i)^2}\left[\sigma_i(L+\sigma_i) - (k\bar{u})^2\right]\overline{\eta'^2}$$

$$(K^T)_{yz} = \frac{G\bar{\mu}}{(k\bar{u})^2 + (L+\sigma_i)^2}$$

$$\cdot\left\{k\bar{u}(L+2\sigma_i)\overline{i\eta'\xi'} + \left[\sigma_i(L+\sigma_i) - (k\bar{u})^2\right]\overline{\eta'\zeta'}\right\} \qquad (9)$$

This follows from the derivation of *Strobel* [1981], with the additional assumption that the radiative damping time scale is much longer than the dynamical time scale. Note that (9) differs from those in *Garcia and Solomon* [1983] and *Smith et al.* [1988] in that wave transience is included (i.e., $\sigma_i \neq 0$). Since the vertical gradient of $\bar{\theta}$ is so large relative to the horizontal, the second term cannot be neglected even though $\overline{\eta'^2} >> \overline{\eta'\zeta'}$ for Rossby waves. To estimate this quantity, we need to know $\overline{\eta'\zeta'}$ and $\overline{i\eta'\zeta'}$. The simplest approximation, made by Newman et al., is that mixing is along zonally averaged potential temperature surfaces, giving $K_{yz} = K_{zy} = [(\partial\bar{\theta}/\partial y)\,(\partial\bar{\theta}/\partial z)^{-1}]\,K_{yy}$; substituting the definitions of displacements (4) then gives $\overline{\eta'\zeta'} \approx [(\partial\bar{\theta}/\partial y)\,(\partial\bar{\theta}/\partial z)^{-1}]\,\overline{\eta'^2}$, with $\overline{i\eta'\zeta'}$ neglected. Using this in (9) and (2) results in a complete cancellation of the contribution to $\overline{v'\mu'}$ due to temperature dependent photochemistry, as one would expect from the assumption that motion occurs along isotherms.

Including eddy variations in temperature and making use of the hydrostatic and adiabatic thermodynamic equations, we can derive expressions that relate $\overline{\eta'\zeta'}$ and $\overline{i\eta'\zeta'}$ to $\overline{\eta'^2}$, for steady conditions ($\sigma_i = 0$)

$$\overline{\eta'\zeta'} = -\frac{1}{S}\left[\frac{f\bar{u}}{2R} + \frac{\partial\bar{T}}{\partial y}\right]\overline{\eta'^2}$$

$$\overline{i\eta'\zeta'} = \frac{Hmf\bar{u}}{RS}\,\overline{\eta'^2}$$

where S is the static stability $[S=\bar{T}/\bar{\theta}(\partial\bar{\theta}/\partial z)]$ and m is the vertical wave number of the Rossby wave, which is calculated as a by-product of the Rossby wave parameterization. These were used in calculations of the role of temperature dependence in the eddy transport of chemically active species presented in section 4.1.

3. Gravity Wave Chemical Eddy Transport

The model uses an adaptation of *Lindzen's* [1981] parameterization for the interaction of breaking gravity waves with the mean flow, described by *Brasseur and Hitchman* [1987]. That parameterization is based on the assumption that, when the wave amplitude becomes sufficiently large to become convectively unstable, the turbulence generated by unstable overturning will act to keep the wave amplitude from growing further with height. The turbulence necessary to maintain a constant amplitude gives the vertical diffusion coefficient, and the constant amplitude assumptions gives the vertical momentum flux divergence that drives the mean circulation. Using this parameterization in its simplest form, $K = K_{zz} = D$, where D is the diffusion coefficient given by Lindzen.

There are two sources of vertical eddy heat transport: turbulent motion and the flow associated with the gravity wave itself. The total transport associated with the gravity wave is given by $-D(\partial\bar{\theta}/\partial z) + \overline{w'\theta'}$, where the primes indicate wave fields. *Schoeberl et al.* [1983] pointed out that the vertical heat flux divergence due to dissipating gravity waves could be expressed in terms of the parameterized turbulent eddy diffusion coefficient. Chemical tracers, like heat, should be transported vertically due to the assumed turbulence, with transport coefficient D, and should also undergo vertical transport due to flow through the dissipating gravity wave. Following *Schoeberl et al.* [1983], we use D' to represent the effective transport coefficient that results from the wave structure; from the notation above, $D' = -\overline{w'\theta'}/(\partial\bar{\theta}/\partial z)$. The effective total transport coefficient is then $K_{zz} = D + D'$.

The transport coefficients for heat (potential temperature) and for trace chemical species are derived from the respective wave equations, and differ only in that the production/destruction rates are different. *Strobel* [1981] presented general expressions for eddy transport including a number of processes such as wave transience and variations in the photochemical lifetime with temperature. *Schoeberl et al.* [1983] apply the assumptions of the Lindzen parameterization to the general expressions of Strobel to derive a form of eddy diffusion for trace species that is straightforward to use with the gravity wave parameterization. They included the turbulent diffusion in the eddy equation used to derive D'.

$$\left(\frac{\partial}{\partial t} + \bar{u}\frac{\partial}{\partial x}\right)\mu' + v'\frac{\partial\bar{\mu}}{\partial y} + w'\frac{\partial\bar{\mu}}{\partial z} = -L\mu' - \overline{GT'}\bar{\mu} + \frac{1}{\rho}\frac{\partial}{\partial z}\left(\rho D\frac{\partial\mu'}{\partial z}\right) \qquad (10)$$

Equation (10) also applies to potential temperature, with μ replaced by θ and the appropriate damping rate used. With the assumptions that the vertical wave number of μ' is the same as that of the gravity wave γ, and that $\gamma >> 1/H$, this can be approximated by

$$\left(\frac{\partial}{\partial t} + \bar{u}\frac{\partial}{\partial x}\right)\mu' + v'\frac{\partial\bar{\mu}}{\partial y} + w'\frac{\partial\bar{\mu}}{\partial z} = -(L + \gamma^2 D)\mu' - GT'\bar{\mu} \qquad (11)$$

L in the formulae from *Strobel* [1981] is replaced by $L+\gamma^2 D$. *Schoeberl et al.* [1983] made the additional approximation that $L >> (k\bar{u}+\sigma)$, i.e., that the time for flow through a gravity wave is short compared to the chemical lifetime of transported species. That assumption was also made by *Garcia and Solomon* [1985], who derived the chemical eddy transport from the chemical eddy continuity equation in the form of (6) rather than (11), i.e., they did not include turbulent diffusion in the budget of μ'. The assumption that the chemical lifetime is long compared with the gravity wave dynamical time scale is valid in most regions for most species, and in those regions the chemical eddy contribution to the gravity wave transport is small. At this point we do not make the assumption of short gravity wave advection time, but will evaluate this in the results.

The expression for D' does not explicitly include wave transience; rather, all dispersive motion is combined into the general category of turbulence and is included in D. The complete form of D', including turbulent diffusion, is

$$D' = \frac{L+\gamma^2 D}{(k\bar{u}+\sigma)^2+(L+\gamma^2 D)}(k\bar{u}+\sigma)^2\overline{\zeta'^2} \quad (12)$$

The effect of temperature dependent reaction rates is given by

$$\left(K^T\right)_{zz} = \frac{G\bar{\mu}}{(k\bar{u}+\sigma)^2+L^2}(k\bar{u}+\sigma)^2\overline{\zeta'^2} \quad (13)$$

where, as for Rossby waves, the radiative damping time is assumed to be much longer than the dynamical time scale. Note that both D' and $(K^T)_{zz}$ require a knowledge of the zonal wave number k. In our implementation of the parameterization [*Brasseur and Hitchman*, 1987] we use a single tunable factor A, which is proportional to ek, where e is the efficiency factor (representing the fraction of time that breaking gravity waves are present). With A specified, a small k implies a larger efficiency factor, and vice versa. The magnitude of A at the boundary was selected so that the parameterized mean flow driving matched that derived from Limb Infrared Monitor of the Stratosphere (LIMS) observations. A value of $k = 2\pi/1000$ km^{-1} was used for the results shown in the following sections; it implies an efficiency factor of $\lesssim 0.1$.

For potential temperature, L and G can be neglected in (12) and (13). When the vertical wavelength of the gravity wave is short $\gamma >> 1/(2H)$, D' reduces to $D/2$, as found by *Schoeberl et al.* [1983]. They also derived the other three components of the K matrix, which are nonzero only if the gravity wave is assumed to have a component in the meridional plane. These additional transport terms are neglected in our model.

Several studies have examined the relationship between the heat flux derived using the assumptions of the Lindzen parameterization and that determined from numerical models of a breaking gravity wave. An important result, supported by several studies [*Chao and Schoeberl*, 1984; *Fritts and Dunkerton*, 1985; *Coy and Fritts*, 1988; *Schoeberl*, 1988] is that the net transport is substantially less than that derived using D. The amount of decrease depends on the degree to which the turbulence generated by convective instability is confined to that part of the wave in which the instability occurs. A greater degree of localization of turbulence gives a weaker heat flux. This reduction factor has been identified in some cases as an inverse Prandtl number. A smaller value of turbulent diffusion is also supported by observations of the mesospheric mean state [*Strobel et al.*, 1985]. To represent this turbulence localization in our model we multiply the derived transport coefficient by a factor of 0.3, which is within the range of the values predicted. Finally, we have $K_{zz}=0.3(D+D')$, where D is derived from the Lindzen parameterization and D' is given by (12). K_{zz} for temperature is the same as that for species μ except that L in (12) is set equal to zero and (13) is omitted.

4. Chemical Eddy Transport Coefficients

4.1. *Meridional Transport Coefficient by Rossby Waves*

This section presents the meridional and vertical eddy transport coefficients for the 2D model, and shows how the net eddy transport changes when the chemical eddy effect is included. The role of the chemical eddy transport in the budget of trace species and the impact of variations in the chemical eddy flux on the simulated model fields are shown in section 5. There are 23 transported species and families in the model and, as expected, there is a large amount of variability in the importance of eddy transport in the budget of the family. Table 1 lists the constituents included. Presentation of results will concentrate on a few species and families of particular interest (e.g., odd oxygen) and on several that are representative of the general pattern.

TABLE 1. Transported Species and Families

Individual Species	Families
N_2O	$NO_y = NO + NO_2 + N + HNO_3 + N_2O_5 + NO_3 + HO_2NO_2 + ClONO_2$
CCl_4	$Cl_x = Cl + ClO + HOCl + ClONO_2 + HCl$
$CFCl_3$	$O_x = O + O(^1D) + O_3$
CF_2Cl_2	
CH_3CCl_3	
CH_3Cl	
CH_4	
C_2H_2	
C_2H_6	
C_3H_8	
HCN	
CH_3CN	
H_2O	
H_2	
CO	
CO_2	
HNO_3	
N_2O_5	
H	

For the calculations presented here, the model was run for 4 years with K_{yy} and K_{zz} determined from the *Hitchman and Brasseur* [1988] and *Lindzen* [1981] parameterizations respectively (i.e., with the same transport coefficients used for all species). This initial run allows the model fields to come into equilibrium. Those model fields are then used to calculate the parameterized transport coefficients using the chemical eddy contribution, so that the relative impact of this model addition on the transport can be assessed. Figure 1 shows K_{yy} computed for pv averaged over the month of January. For this

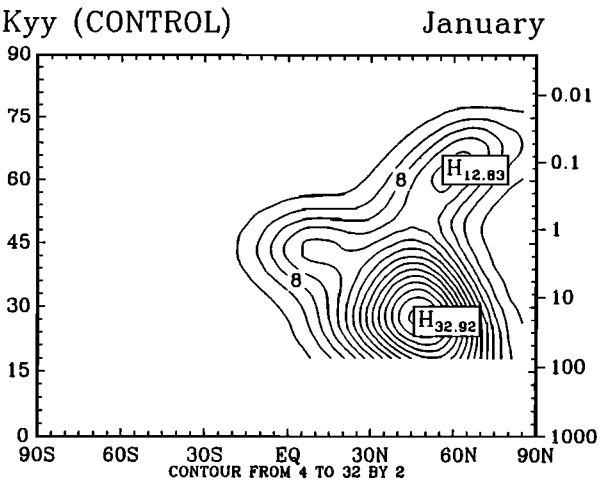

Fig. 1. Control (species independent) meridional eddy transport coefficient (K_{yy}) for January. Units are 10^5 m^2 s^{-1}.

period, K_{yy} has a peak in the lower stratosphere in the northern hemisphere with moderately large values extending to the upper stratosphere tropics and the high latitude mesosphere. K_{yy} is small throughout the summer extratropics. K_{yy} for pv and for all trace species is restricted to be at least 3×10^5 m^2 s^{-1} for reasons of numerical stability.

In calculating the chemical eddy transport coefficient from $(K^q)_{yy}$ there is some flexibility within the constraints imposed by the wave parameterization and the form of the chemical eddy representation. The *Hitchman and Brasseur* [1988] Rossby wave parameterization specifies a total wave activity damping α. In the present study, α at individual gridpoints can be modified based on the local mean gradient of potential vorticity, as described in section 2.2. From (8) there is a damping L_q and an effective dissipation due to wave transience σ_i. Equating the total effective loss rates gives $\alpha = L_q + \sigma_i$. Although the sum (α) is specified, no additional constraints on either L_q or σ_i are provided by the parameterization. As evidence in (8), the relative magnitude of L_q and σ_i can affect the relationship between $(K^q)_{yy}$ and $(K^\mu)_{yy}$. We choose two different options that illustrate how transport of trace species and pv are related under different conditions.

In the first series of calculations $L_q = \alpha$, $\sigma_i = 0$. This is, in effect, an assumption that dispersion does not play a role in the transport of pv or trace species; rather, all violation of the non-acceleration conditions and associated pv transport is due to explicit damping of wave activity. In the second assumption, $L_q = L_{rad}$ and $\sigma_i = \alpha - L_{rad}$. Again the total $(L_q + \sigma_i)$ is the same, and therefore $(K^q)_{yy}$ does not change. The different value of σ_i affects the relative magnitude of $(K^\mu)_{yy}$ and $(K^q)_{yy}$. In this second assumption, the only damping that acts selectively on pv is that due to radiative processes (parameterized based on a mean damping of temperature in the form of Newtonian cooling); all other effects that contribute to pv transport (e.g., transience, nonlinearity) can also act to transport trace chemical species. L_{rad} is computed from a smoothed curve fit to the height-dependent Newtonian cooling coefficient computing from LIMS data by *Gille and Lyjak* [1986]. Letting b represent the Newtonian cooling rate (thermal damping)

$$L_{rad} \cdot q = \frac{\kappa}{R} \frac{f}{\rho} \frac{\partial}{\partial z} \left(\rho \frac{bT}{S} \right)$$

Neglecting variations of b with height, then L_{rad} is related to b by the ratio of the vertical structure component of potential vorticity to the total potential vorticity, which is normally much less than one. We use the upper limit ($L_{rad} = b$), which is a function of height only. Since the calculation is insensitive to the structure or magnitude of L_{rad} as long as $L_{rad} << \alpha$, the impact of this simplification is minor.

The two different sets of assumed values for L_q and σ_i represent two extremes within the constraint imposed by the wave drag parameterization (i.e., $L_q + \sigma_i = \alpha$), and can give an indication of how the nature of the pv transport affects the transport of trace constituents. Neither assumption is very realistic, and therefore choosing which is most like the atmosphere is difficult. The most severe problem is the use of a specified height-dependent profile of α. While the assumption that the wave damping due to diabatic effects is roughly linear may be an adequate approximation, there is no reason to expect that other processes that give pv transport can in general be represented by an additional linear damping. Evidence from observations [e.g., *McIntyre and Palmer*, 1983] and numerical models [*Plumb and Mahlman*, 1987] indicates that there is enhanced mixing in the low latitude region where the vorticity gradient is weaker. A crude representation of this has been incorporated in the model by increasing α at gridpoints for which $\partial\bar{q}/\partial y \le 0$. A more realistic variation of σ_i with the circulation conditions, either interactively or based on climatology, would be desirable. That refinement has not been included in the present study, which is focussed only on the transport of trace constituents.

Four species or families are used to illustrate the dependence of K_{yy} on chemistry: O_x, HNO_3, N_2O, and N_2O_5. The O_x family consists of O_3, O, and $O(^1D)$, and is dominated by O_3 in the stratosphere. Both O_x and HNO_3 have transition regions in the stratosphere, where their photochemical time scale is close to the zonal advection time scale, and are therefore expected to experience enhanced transport there. Global measurements of both have been made [e.g., *Gille*, 1987], and meridional fluxes derived from observations can be used for comparison. N_2O has a slow destruction rate and tropospheric origin; its behavior is similar to many of the so-called source gases, including the chlorofluorocarbons. The other extreme is provided by N_2O_5, which undergoes rapid

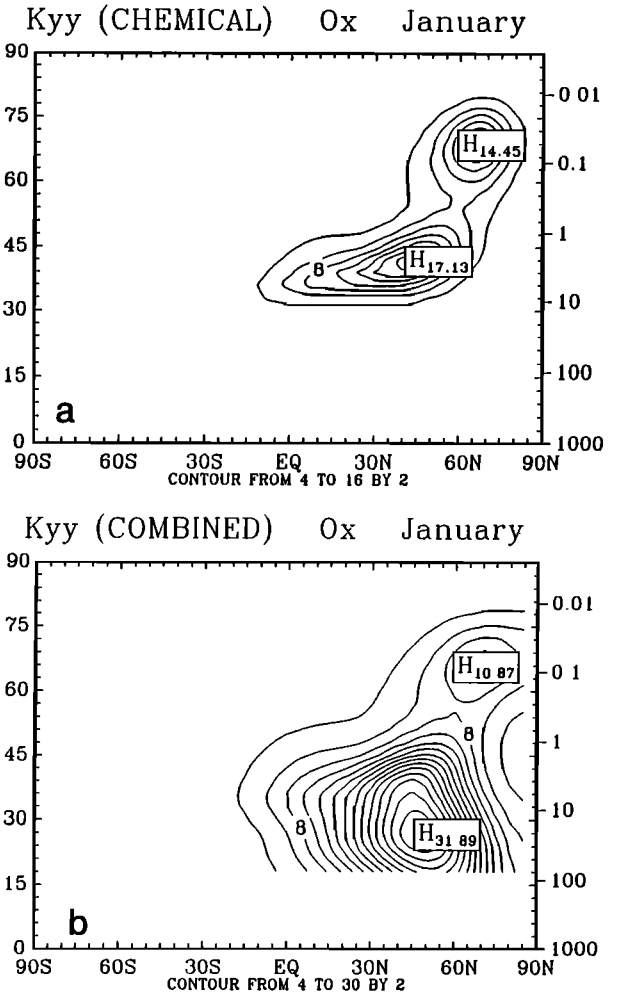

Fig. 2. Meridional eddy transport coefficient (K_{yy}) for January for odd oxygen (O_x) computed from the chemical eddy parameterization with the assumptions of (*a*) no wave transience and (*b*) large wave transience. See text for details. Units are 10^5 m^2 s^{-1}.

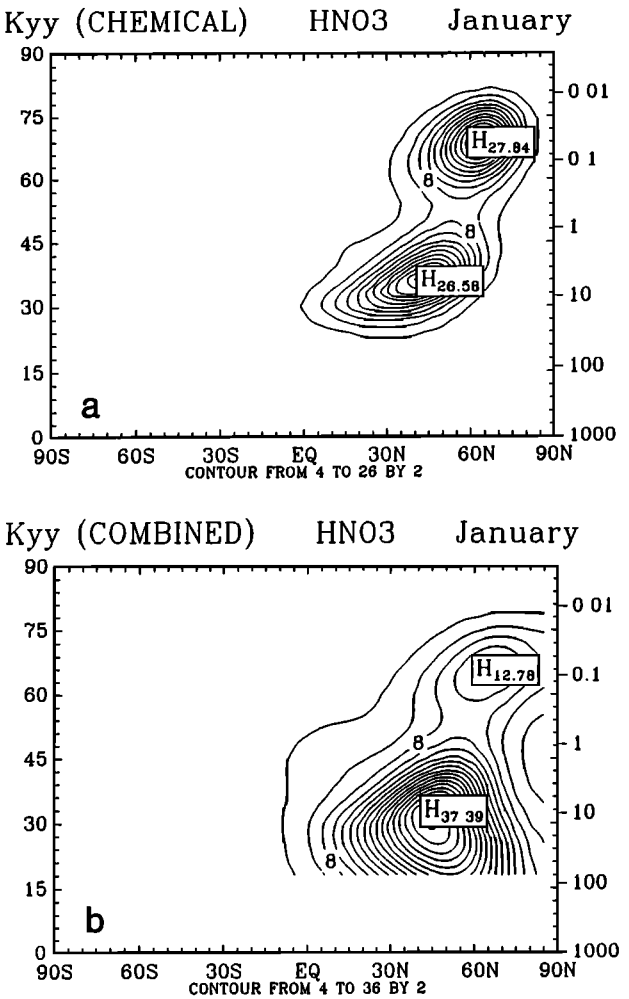

Fig. 3. As in Figure 2, but for nitric acid (HNO_3).

photochemical destruction. Figure 2-5 show $(K^{\mu})_{yy}$ computed from $(K^{q})_{yy}$ using the two different assumptions described above for each of these four species. In the upper panel (a) of each plot K_{yy} has been calculated from the first assumption ($L = \alpha$, $\sigma_i = 0$), which, in effect, assumes that there is no transience or dispersion.

The photochemical lifetimes for O_x and HNO_3 are substantially longer than the dynamical advection time in the lower stratosphere, so as a result the chemical eddy K_{yy} is small there (Figure 2*a* and 3*a*). The dynamical and chemical time scales are comparable in the middle and upper stratosphere and there K_{yy} for these two species is the same order as that for pv. In the mesosphere, the damping rate for pv (L_q) is quite large due to an imposed sponge layer in the parameterization [*Hitchman and Brasseur*, 1988]. So, for example, at 70 km the lifetime for pv is about 0.1 day. In comparison, the lifetime for O_x has strong latitudinal variations, but at 60° N is about 1 day. From (8) it is evident that for $L_q >> L_{\mu}$ and $L_{\mu} \gtrsim k\bar{u}$, the transport coefficient for μ will be greater than that for pv. The peak in K_{yy} for O_x and certain other species depends on the very large decay rate for pv, which is specified in the model to prevent wave activity from approaching the model upper boundary. The large damping rate receives support from observational evidence that planetary waves in the mesosphere are perpetually "breaking" and that pv is not conserved to the resolution of the observations [*Dunkerton and Delisi*, 1985; *Schoeberl and Smith*, 1986]. In any event, this mesospheric K_{yy} maximum occurs only for species with relatively short decay time scales there. Because it affects transport only for species that are under photochemical control, its impact on the zonal mean distributions of trace species is negligible.

In contrast to O_x and HNO_3, N_2O (Figure 4*a*) has a relatively long lifetime in the stratosphere. From (7), with $\sigma_i = 0$, K_{yy} is roughly proportional to L_{μ}, which is small. The tropical maximum in K_{yy} for N_2O results from the fact that the dynamical time scale is much longer here than in high latitudes due to the weak zonal wind speed and the larger distance around the globe. Therefore a transition region, where dynamical and chemical time scales are comparable, exists for N_2O, a constituent that would not normally have a large chemical eddy contribution to transport in the winter stratosphere. This tropical maximum in K_{yy} is seen in a number of other species with moderately slow photochemical destruction rates.

A third type of behavior is seen in Figure 5*a*, which shows K_{yy} for N_2O_5. For this species the photochemical loss time is short, and the transition region is located in the lower and middle stratosphere.

The assumption made in producing the lower panels b of Figures 2-5 is the second one, that the damping that is specific to wave activity is due to radiative processes only, so that (α =

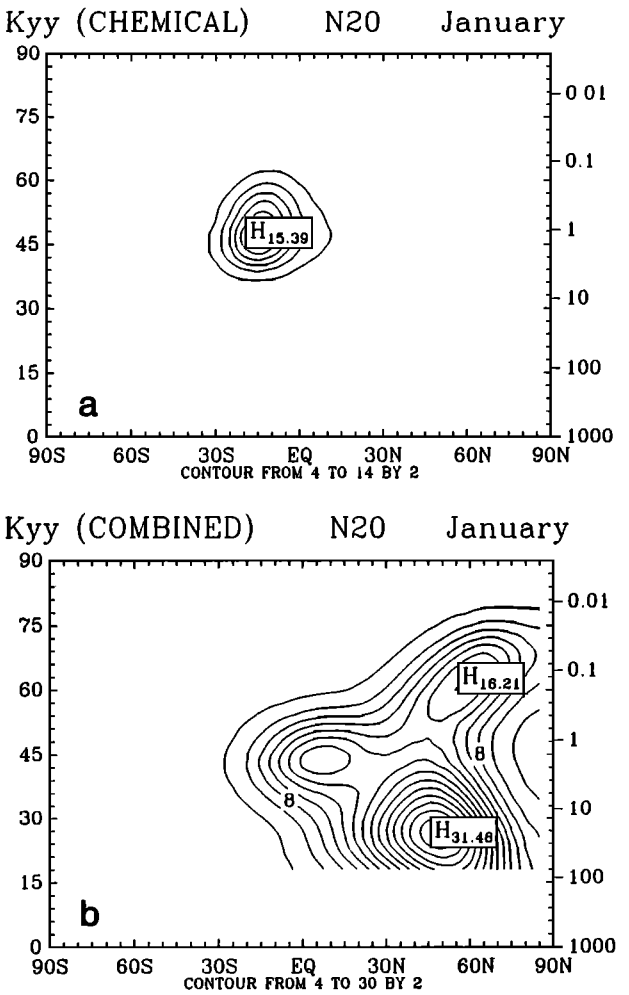

Fig. 4. As in Figure 2, but for nitrous oxide (N_2O).

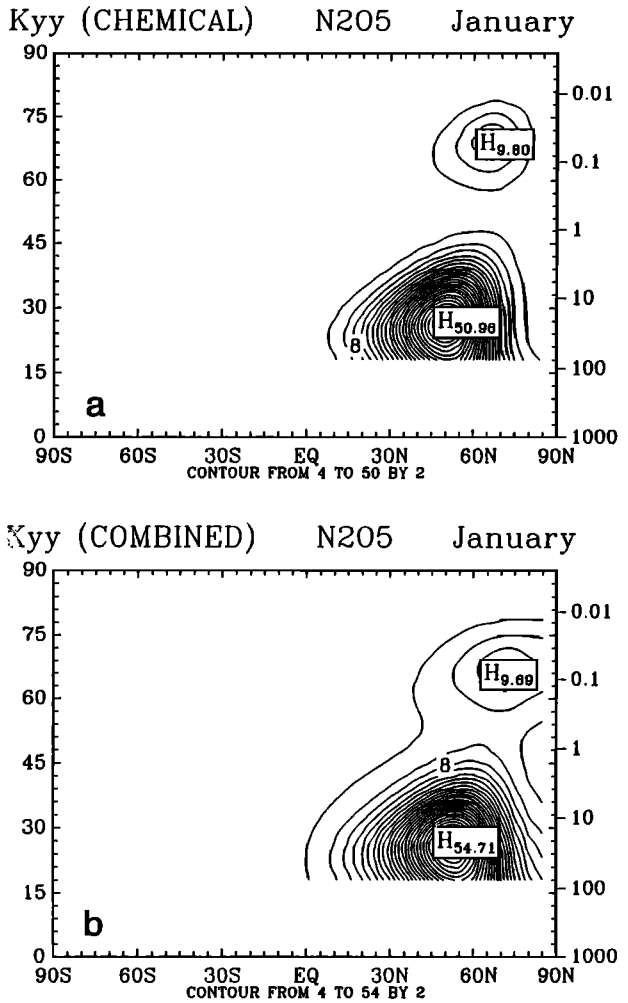

Fig. 5. As in Figure 2, but for dinitrogen pentoxide (N_2O_5).

$L_{rad} + \sigma_i$). From (8), it is evident that since L_{rad} is small, then for species with long lifetimes ($L_\mu << \sigma_i$), $(K^\mu)_{yy}$ will be similar in structure to $(K^q)_{yy}$. This is clearly seen in K_{yy} for N_2O (Figure 4*b*). The magnitudes of $(K^\mu)_{yy}$ for odd oxygen and nitric acid (Figures 2*b* and 3*b*) are larger in the lower stratosphere than they were with the previous (damping dominated) case, but are smaller in the lower mesosphere. The transport coefficient for N_2O_5 (Figure 5*b*) is similar in both cases; for this species, $L_\mu >> \sigma_i$ even with the large value of σ_i, so photochemistry controls the eddy transport.

Smith et al. [1988] showed that the temperature dependence of the reaction rate can make a substantial contribution to ozone transport. Figure 6 shows the meridional transport of O_x by Rossby waves due to K_{yy}, that due to the temperature dependent contribution, and the sum. The temperature dependence was computed from (9) with the contribution from the asymmetric part of K_T (the $i\eta'\zeta'$ term) neglected. The temperature dependence of the ozone destruction rate changes not only the magnitude but also in some places the sign of the ozone flux in the transition region (30-40 km).

4.2. *Vertical Transport Coefficient by Gravity Waves*

The relevant quantity for the parameterized gravity wave transport in the model is the net vertical transport coefficient, which includes turbulent transport, wave transport and the adjustment for the localization of turbulent diffusion. The combined transport coefficients $K_{zz} = 0.3(D+D')$ are presented here.

Calculation of K_{zz} show that it is almost identical to that calculated for a conserved tracer (with $L = 0$ in (12)) or heat (assuming wave motion is adiabatic) for most families in our model. In other words, the vertical transport coefficients for

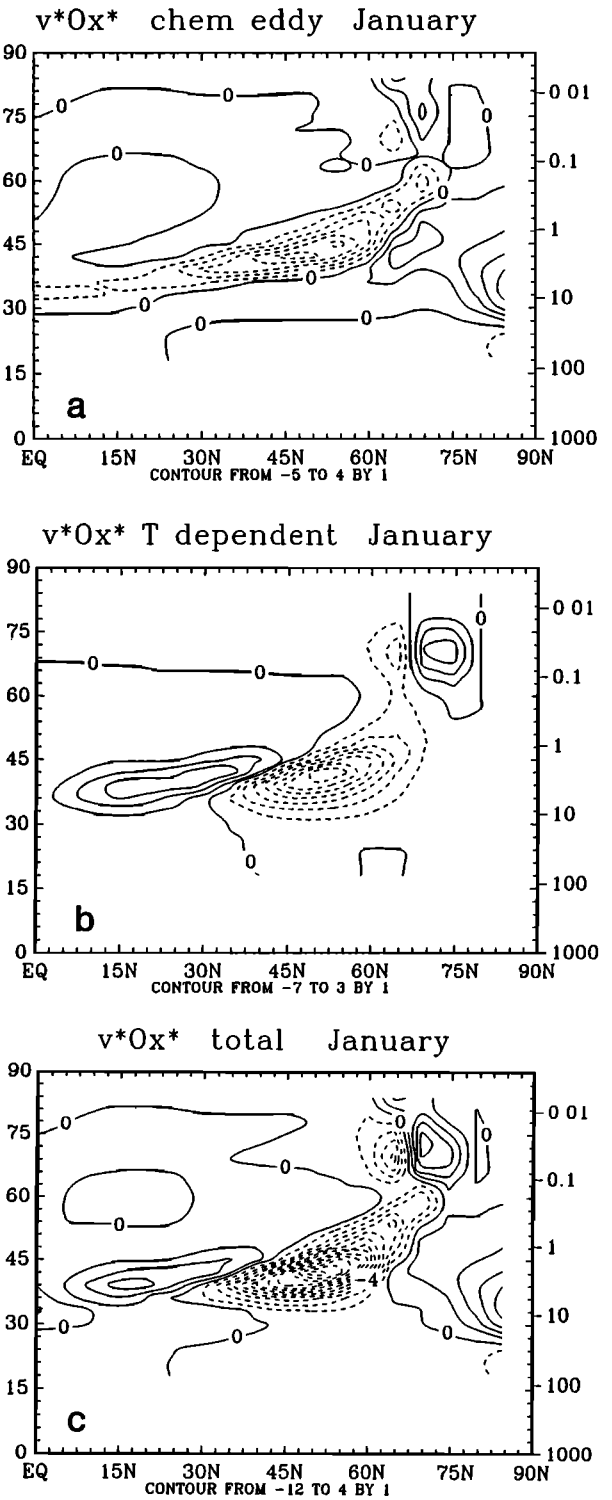

Fig. 6. Chemical eddy parameterization of the meridional flux of odd oxygen computed from (*a*) $\overline{v\mu'} = (K^\mu)_{yy}(\partial\,\bar{\mu}/\partial y)$, (*b*) $\overline{v\mu'} = (K^T)_{yy}(\partial\bar{\theta}/\partial y) + (K^T)_{yz}\,\bar{T}/\bar{\theta}\,(\partial\bar{\theta}/\partial z)$, and (*c*) the sum.

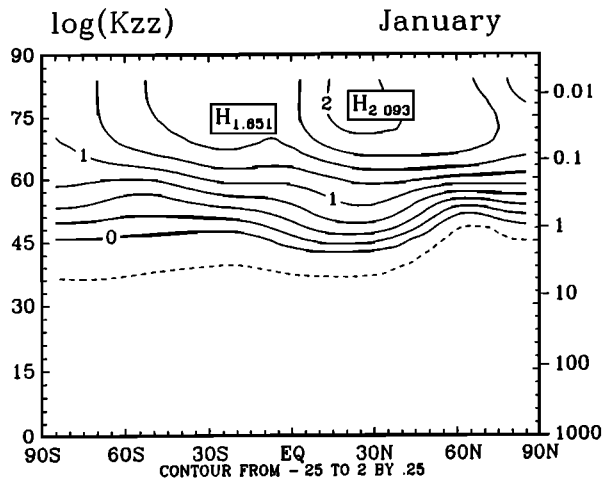

Fig. 7. Log of control (species independent) vertical eddy transport coefficient (K_{zz}) for January. Units are $m^2 s^{-1}$.

heat and those for trace constituents are the same. It is also valid to adopt the approximate form of K_{zz} given by *Schoeberl et al.* [1983] and *Garcia and Solomon* [1985] (i.e. assuming that $L_\mu << k\bar{u}$) because the combined dynamical and turbulent transport time scale is much less than the photochemical damping time. However, it is almost as accurate to neglect the chemical eddy transport altogether and use the D' derived for heat (the control) for all species. Figure 7 shows K_{zz} for heat, and Figure 8 shows that for O_x. K_{zz} for O_x is quite similar to that for heat; for most other species the differences between the chemical eddy and control K_{zz} are even smaller. *Strobel et al.* [1987] also found that the photochemical acceleration of the eddy transport by gravity waves was negligible for all species except O and O_3. They found much larger differences between K_{zz} of O_x and that of temperature than found in the present study, which can be attributed to their neglect of the $\gamma^2 D$ term in (12). Since $\gamma^2 D$ is much greater than L_μ, it has the effect of reducing the impact of the photochemical acceleration on transport.

The only other species or family for which there is any significant variation in K_{zz} due to the chemical eddy effect is atomic hydrogen H, which is controlled by photochemistry and

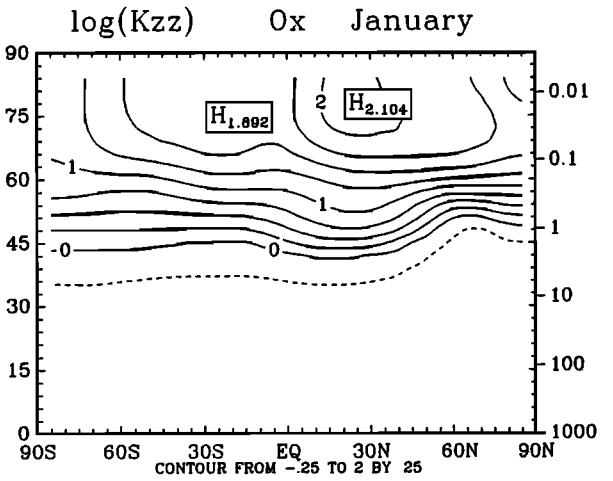

Fig. 8. Log of vertical eddy transport coefficient (K_{zz}) for January for odd oxygen (O_x) computed from the chemical eddy parameterization. Units are $m^2 s^{-1}$.

is relatively insensitive to K_{zz}. Even for H, which has a very rapid loss rate, the change in K_{zz} due to the inclusion of the chemical eddy contribution to gravity wave transport are moderate (<10%). Overall, it appears that the chemical eddy contribution to gravity wave transport can be neglected without much impact on the results. The contribution of the temperature dependent reaction rates is even smaller.

The relatively small role played by chemistry in the parameterized vertical eddy transport is to some extent built into the model and may not correspond to its actual role in the mesosphere. The family approach is used to solve for trace species. In this formulation, species are grouped into several families that have relatively long lifetimes. Short-lived species are determined using photochemical equilibrium theory. It is these equilibrium species for which the chemical time scale is most likely to be close to the advection and turbulent time scales, and consequently the chemical eddy contribution to the gravity wave transport is most likely to be significant when compared to the turbulent transport. However, it is also true that over the long time scales that we are concerned with in this model, those short-lived species are not very sensitive to eddy transport, and therefore even a large variation in K_{zz} may have only an insignificant effect on the total budget.

5. Importance of Chemical Eddy Transport in Budgets of Trace Species

Even where the transport coefficient computed using the chemical eddy contribution differ substantially from the control (species independent) transport coefficients, this will not be important in the model simulations unless the species distribution is sensitive to the eddy transport. This section considers the direct role of the variations in the eddy transport on the budget of trace species in the model and the changes in the distributions due to variations in the K_{yy} and K_{zz} formulation.

The processes tending to change the concentration of tracer μ can be separated into four terms

$$\frac{\partial \bar{\mu}}{\partial t} = \underbrace{-\bar{v}^* \frac{\partial \bar{\mu}}{\partial y} - \bar{w}^* \frac{\partial \bar{\mu}}{\partial z}}_{I} + \underbrace{\bar{P} - L\bar{\mu}}_{II}$$

$$+ \underbrace{\frac{1}{\cos\varphi}\frac{\partial}{\partial y}\left(\cos\varphi K_{yy}\frac{\partial}{\partial y}\bar{\mu}\right)}_{III} + \underbrace{\frac{1}{\rho}\frac{\partial}{\partial z}\rho K_{zz}\frac{\partial \bar{\mu}}{\partial z}}_{IV}$$

These contributions will be referred to as I, advection by the mean meridional circulation; II, source term (production minus loss); III, meridional eddy flux convergence; and IV, vertical eddy flux convergence.

Figure 9 shows two plots of the processes acting to vary or maintain the distribution of O_x as a function of latitude over the altitude range 30-35 km during January and February. Curve A corresponds to meridional eddy flux convergence using K_{yy}, curve B to advection by the mean circulation, and curve C to photochemical production and loss. At this level, the computed eddy flux divergence from gravity waves is small for all species, and is not shown. To create Figure 9*a* the control K_{yy} was used for the entire integration (4 years), while in Figure 9*b* the K_{yy} depending on photochemistry due to the chemical eddy effect was used. The case with no mixing ($\sigma_i = 0$),

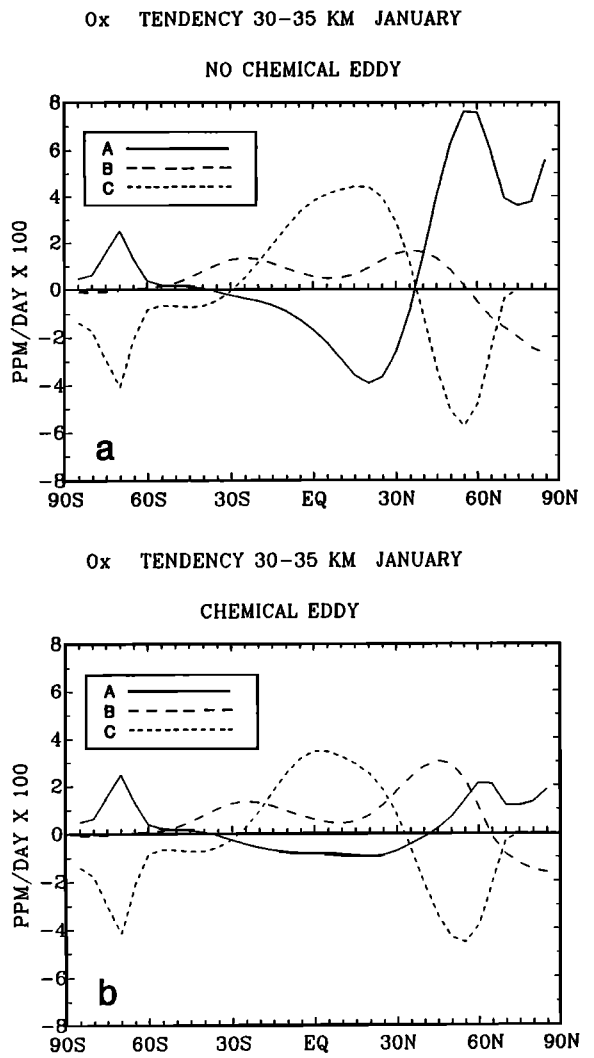

Fig. 9. Tendency terms in the budget of zonal mean O_x for the height range 30–35 km for January. Curve A is meridional eddy transport $\partial[K_{yy}\,(\partial\bar{\mu}/\partial y)]/\partial y$, curve B is advection by the mean circulation $\bar{v}^*(\partial\bar{\mu}/\partial y) + \bar{w}^*(\partial\bar{\mu}/\partial z)$, and curve C is the net production and loss. In making (*a*) the control (species independent) version of K_{yy} was used, and in (*b*) the chemical eddy K_{yy} based on the assumption of no dispersion was used. Units are ppm d^{-1}; values on the ordinate have been amplified by a factor of 100 for plotting.

corresponding to Figure 2a is used for the chemical eddy parameterization here. The case with larger mixing ($\sigma_i = \alpha - L_{rad}$; not shown) is, for most species, closer to the control case (Figure 9*a*).

There are several aspects of the meridional eddy transport that can be seen in Figure 9: the importance of eddy transport relative to other processes in maintaining the ozone distribution; the differences between the meridional eddy transport in the two different integrations; and the differences in the magnitude of zonal mean transport or production/loss rate in the two integrations. The control case indicates that eddy transport, mean transport and photochemistry all play a role in controlling the distribution of O_x in this region. O_x tends to be produced in the tropics and transported toward the winter pole by the meridional eddy flux. Mean advection is small in low latitudes because of the weak vertical gradient near the ozone mixing ratio maximum, but balances the eddy flux in the polar night. Incorporation of the chemical eddy transport leads to significant changes in the balance, most notably a sharp reduction in magnitude of the eddy transport. (The eddy transport in the extratropical Southern Hemisphere is at the default minimum in both cases, and so does not change.) Note that the magnitude of the other two terms shown varies also. In middle Northern latitudes there is a simultaneous decrease in the rate of odd oxygen loss by photochemistry and an increase in its rate of transport by the mean circulation. The combination indicates that an approximate balance is reached, so that the net change in O_x with time is moderate.

The budgets for HNO_3, N_2O and N_2O_5 for the same period are shown in Figures 10–12, respectively. As in Figure 9, the $(K^{\mu})_{yy}$ calculated assuming no pv mixing ($\sigma_i = 0$) is compared with the control. Note that for HNO_3 and N_2O_5 a slightly lower region is presented than shown for O_x and N_2O. HNO_3 has a strong, photochemically driven gradient in high latitudes. (The model includes a conversion of N_2O_5 to HNO_3 in the polar night with a time constant of 20 days, consistent with the analysis of *Evans et al.* [1985].) In this region the budget is altered with the use of the chemical eddy rather than control eddy transport. Figure 10 indicates a factor of 2 decrease in the

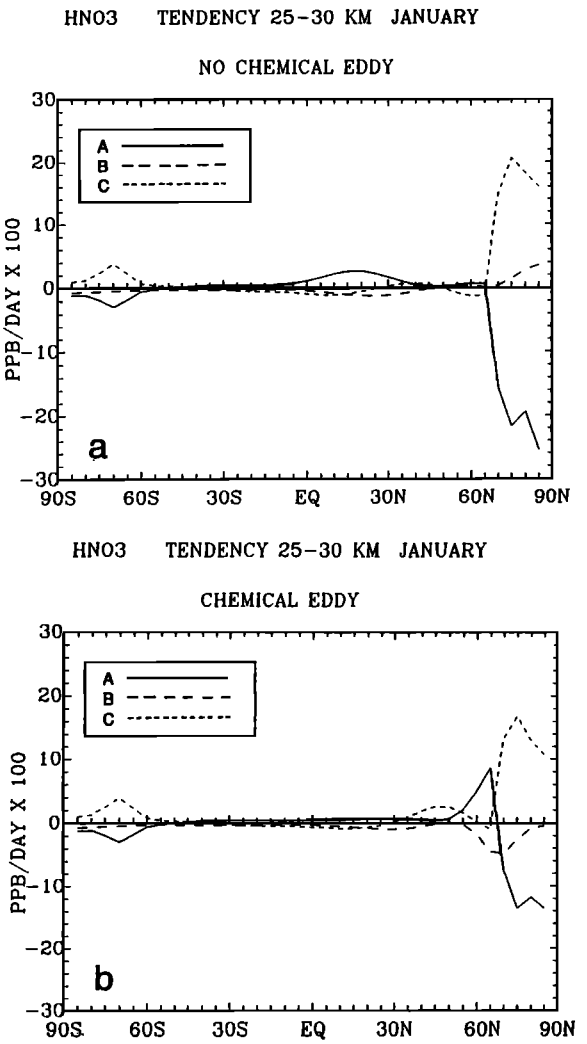

Fig. 10. As in Figure 9, but for HNO_3 and the height range 25–30 km. Units are ppb d^{-1}; values on the ordinate have been amplified by a factor of 100 for plotting.

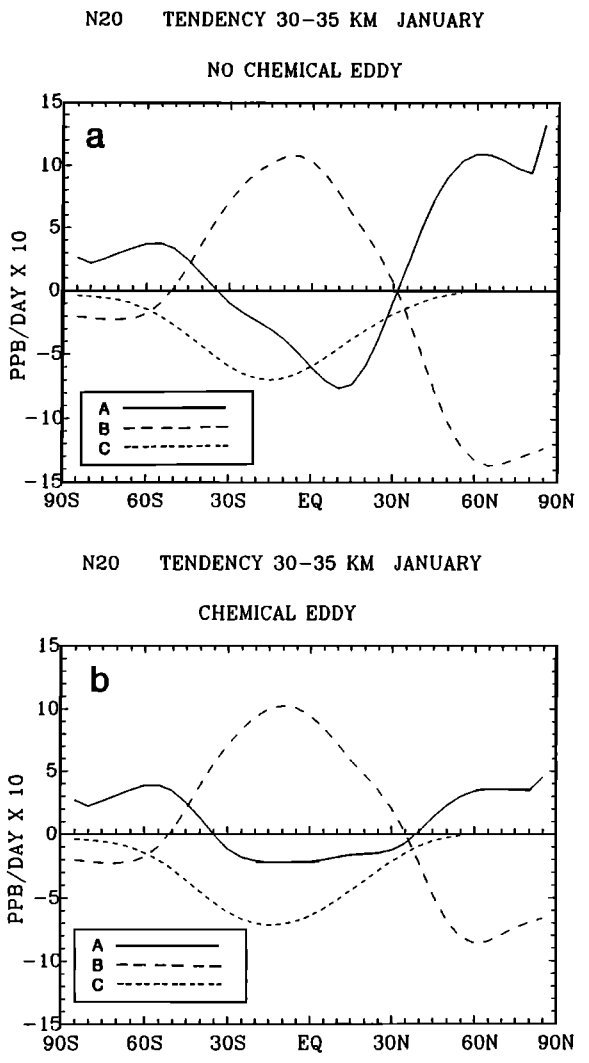

Fig. 11. As in Figure 9, but for N_2O. Units are ppb d^{-1}; values on the ordinate have been amplified by a factor of 10 for plotting.

magnitude of the eddy transport maximum. There is a moderate decrease in the magnitude of the photochemical tendency. The negative correlation between eddy transport and production/loss takes the form of a simple feedback. Decreased transport in the region of the mixing ratio maximum allows the concentration to increase there and to decrease away from there. The destruction rate is proportional to the mixing ratio, and will thus vary with the changes in the transport. Note also that the mean advection has changed in both sign and magnitude; this reflects a shift in the height of the HNO_3 mixing ratio maximum.

N_2O (Figure 11) has a steep vertical gradient, and its distribution is affected by mean vertical advection. In the control case, this is balanced by both eddy transport and photochemical loss in low latitudes, and primarily by eddy transport in high latitudes. When the chemical eddy parameterization is used, there is a strong drop in the magnitude of the eddy transport, as expected from the much lower transport coefficient (Figure 3). There is a weak decrease in the magnitude of the mean advection in low latitudes and a stronger decrease in the high latitude winter. This change is a direct result of changes in the N_2O distribution, since the mean circulation (to be discussed further below) is essentially unchanged in the two integrations.

Unlike the other species shown, the eddy transport coefficient for N_2O_5 increases, rather than decreases, when the eddy transport coefficient is used (Figure 5). Note from Figure 12 that both the eddy transport tendency and the photochemical production/loss tendency increase by about a factor of two with the chemical eddy calculation. For changes in the N_2O_5 mixing ratio to be the cause of the enhanced production in the chemical eddy calculation would signal a very large decrease in the N_2O_5 mixing ratio. Comparison of distributions from the two runs, to be discussed next, do not indicate that this is the case. The probable cause of the increased production will be discussed below.

The final test of the importance of the chemical eddy contribution to transport is an assessment of how it changes the distributions of trace species in long-term model simulations. As shown in the previous section, variations in the eddy transport can change the magnitude or even the sign of other processes in the model through photochemical, dynamical or photochemical feedback.

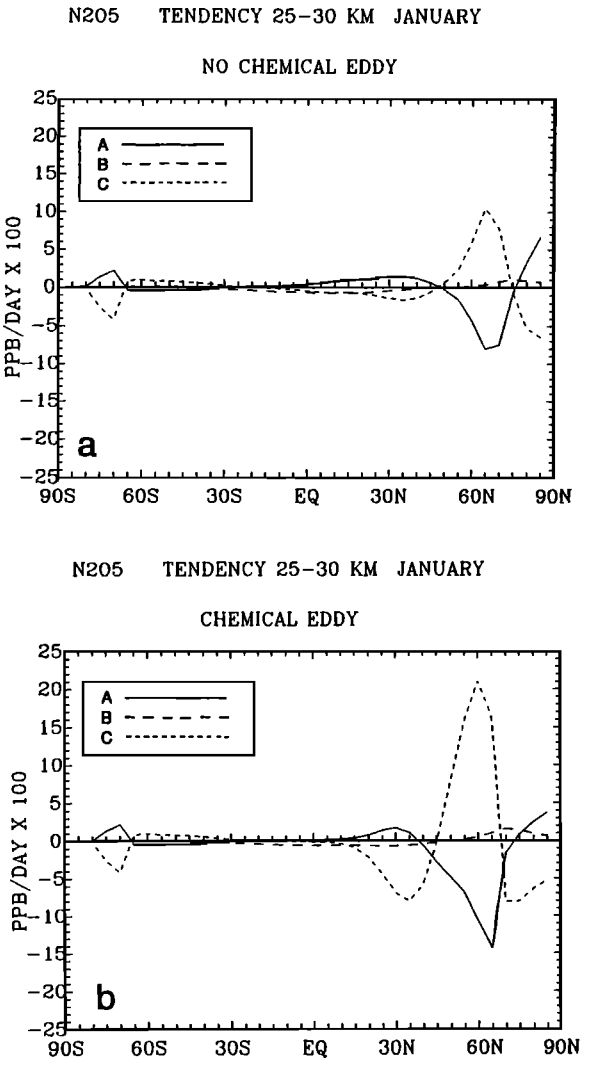

Fig. 12. As in Figure 9, but for N_2O_5 and the height range 25–30 km. Units are ppb d^{-1}; values on the ordinate have been amplified by a factor of 100 for plotting.

Here the distributions of trace species after a four year integration with the control and chemical eddy transports are compared. Although the eddy transport coefficients enter directly only into the continuity equations for trace species, due to feedbacks any of the model fields can change. The feedback of variations in the chemical composition on dynamical fields is weak. The only steps in the model where this occurs are in the absorption of short wave radiation by ozone and in the calculation of infrared transfer due to carbon dioxide, ozone and water vapor. These can both modify the net diabatic heating, which then affects temperature and the mean meridional circulation. The changes in the dynamical fields associated with the K_{yy} modifications shown in this section are quite small ($\lesssim$1 K in temperature and $\lesssim$1 m s^{-1} in zonal wind). Variations in the dynamical transport coefficient K_{yy} are also small ($\lesssim 1\times10^5$ m^2 s^{-1}). The feedbacks through dynamical fields $\bar{u}$, $\bar{T}$, $(K^q)_{yy}$) are sufficiently small that they can be ignored. The changes found with the introduction of the chemical eddy K_{yy} are due to the direct effect of the modified K_{yy} in the chemical continuity equation and to photochemical feedbacks such as the dependence of the production and loss rates of one species on the distribution of another.

Figure 13*a* shows the odd oxygen distribution with the control values for K_{yy} and K_{zz}, Figure 13*b* shows that using the chemical eddy value of K_{yy} (computed using the first assumption of no dispersion), and Figure 13*c* shows the difference. The largest difference is a reduction in the O_x in middle and high northern latitudes in the middle stratosphere (30–3 mbar) when the chemical eddy calculation is used. The chemical eddy value is more realistic although neither integration is successful in reproducing the observed ozone mixing ratio maximum in high latitudes near 3 mbar (see, for example, SBUV January ozone mixing ratios [*McPeters et al.*, 1984].)

Nitric acid is another species for which global observations are available. LIMS data for December and January [*Austin et al.*, 1986] indicate a maximum mixing ratio of ~10 ppb near 20 mbar at the winter pole and a summer maximum of ~7 ppb at a slightly lower level. Both model calculations (Figure 14) give HNO_3 mixing ratios with peak values that are approximately the same as the observed maxima near both poles. Note that the northern hemisphere maximum occurs around 10 mbar in the control run, whereas for the chemical eddy case it is near 30 mbar, lower by about a scale height. This change brings the level of the maximum closer to the observed height of maximum HNO_3. Both of the integrations indicate weak concentrations of HNO_3 in low and middle latitudes, while LIMS observations show that mixing ratios as high as 7 ppb are found at 30° N during December and January.

Figure 15 shows the distribution of N_2O from the two model runs. Recall that N_2O is transported up from the troposphere and undergoes slow destruction in the stratosphere. With the chemical eddy parameterization, the N_2O mixing ratio is decreased in the high-latitude middle and upper stratosphere. These changes are completely consistent with a sequence in which a decrease in K_{yy} leads to decreased transport into the polar stratosphere. The resulting change in the gradient also leads to variations in the advection by the mean meridional circulation. The N_2O distribution can be compared with that for January measured by SAMS [*Jones and Pyle*, 1984]. The observations, like the model run in which the chemical eddy transport is used, indicate a significant meridional gradient in the mid-latitude middle stratosphere. Both model integrations show a somewhat different structure than observed, and, in particular, do not have the region of high N_2O mixing ratio extending upward and poleward on either side of the equator.

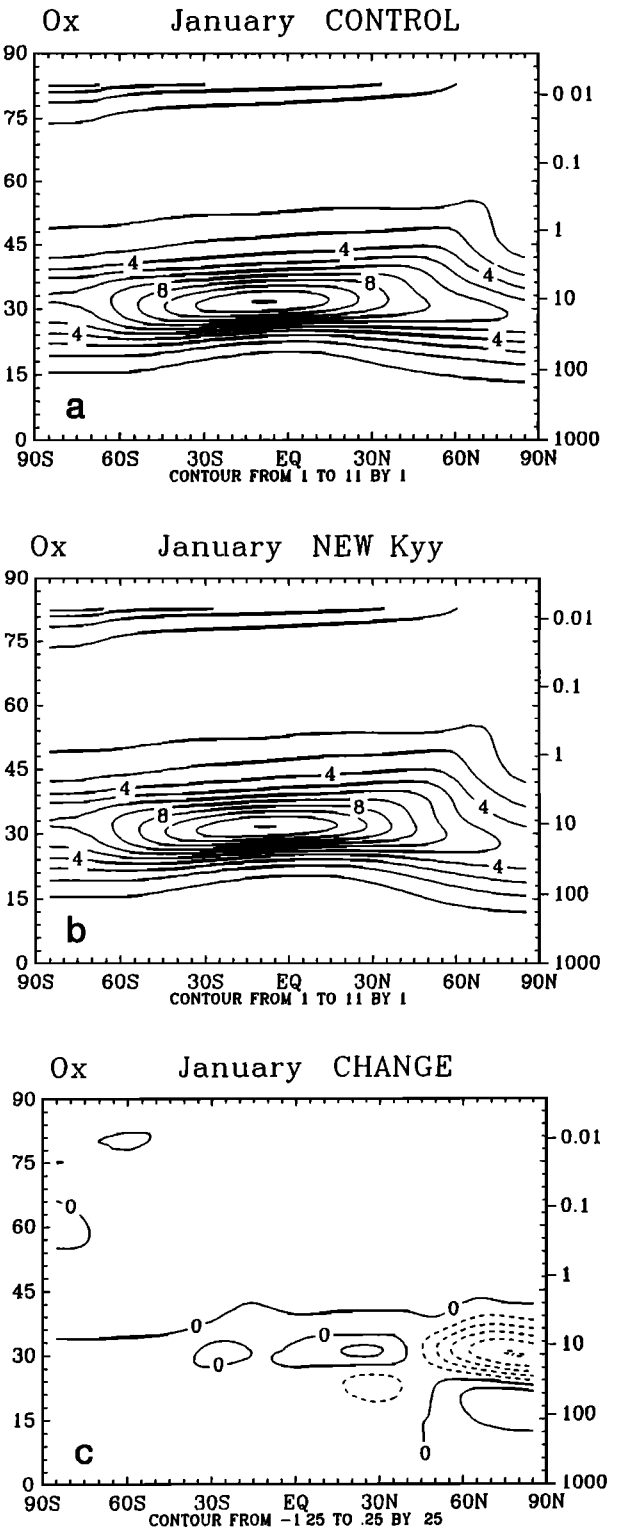

Fig. 13. Zonal mean O_x mixing ratio (ppmv) during January computed using (*a*) the control K_{yy} and K_{zz}, and (*b*) the chemical eddy K_{yy} based on the assumption of no dispersion and control K_{zz}. (*c*) Difference between Figures 13*a* and 13*b*.

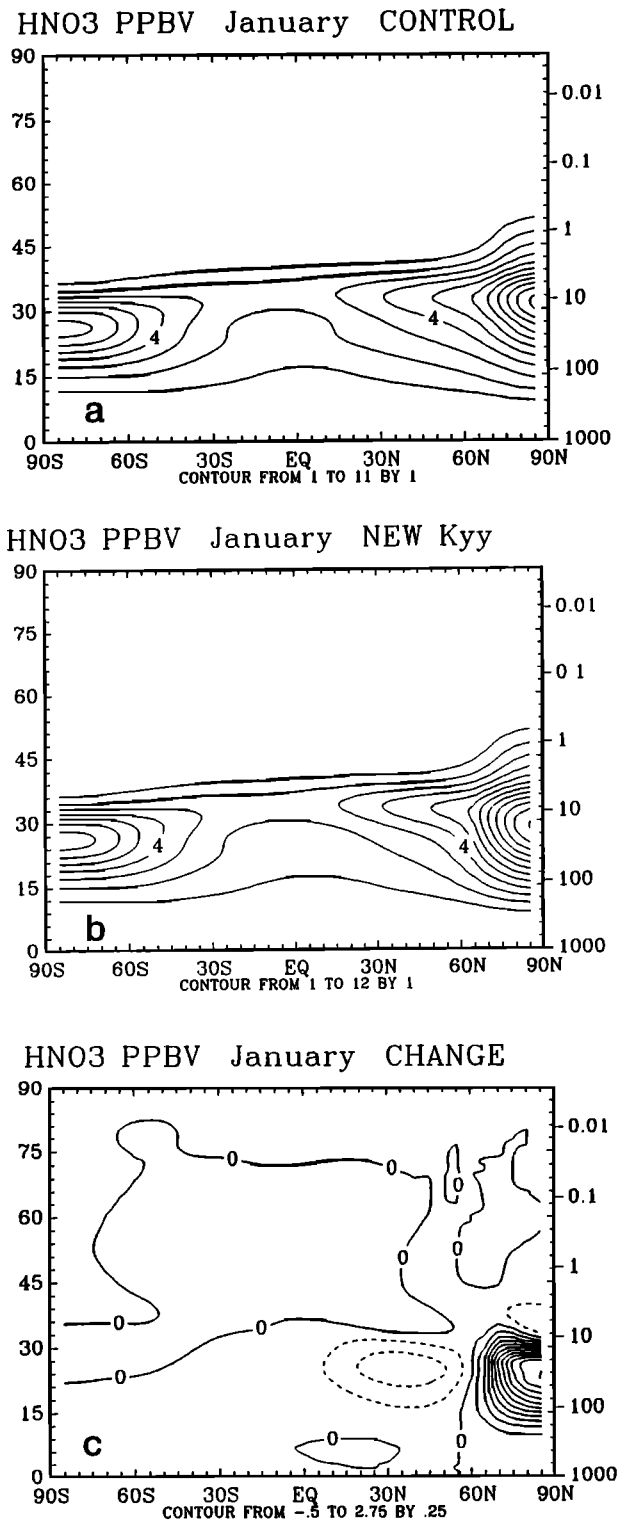

Fig. 14. As in Figure 13, but for HNO_3 mixing ratio (ppbv).

Jones and Pyle attribute this pattern to advection by a two-cell mean circulation.

Figure 16 illustrates the distribution of N_2O_5 from these two model integrations. The change is significant poleward of about 55°N. There is a large increase in K_{yy} when the chemical eddy parameterization is adapted (note peaks at 30 mbar of 33×10^5 m^2 s^{-1} for the control and 51×10^5 m^2 s^{-1} for the chemical eddy transport coefficients.) The reduction using the chemical eddy parameterization can be attributed to two factors. First, the stronger (chemical eddy) K_{yy} transports more N_2O_5 out of the polar region, where it is rapidly destroyed. Thus there is a decrease in high latitudes that is not accompanied by an increase in lower latitudes. Also, production of N_2O_5 depends on the concentration of ozone. With the chemical eddy parameterization, the ozone mixing ratio is reduced (Figure 13) and therefore there is a reduced production of N_2O_5.

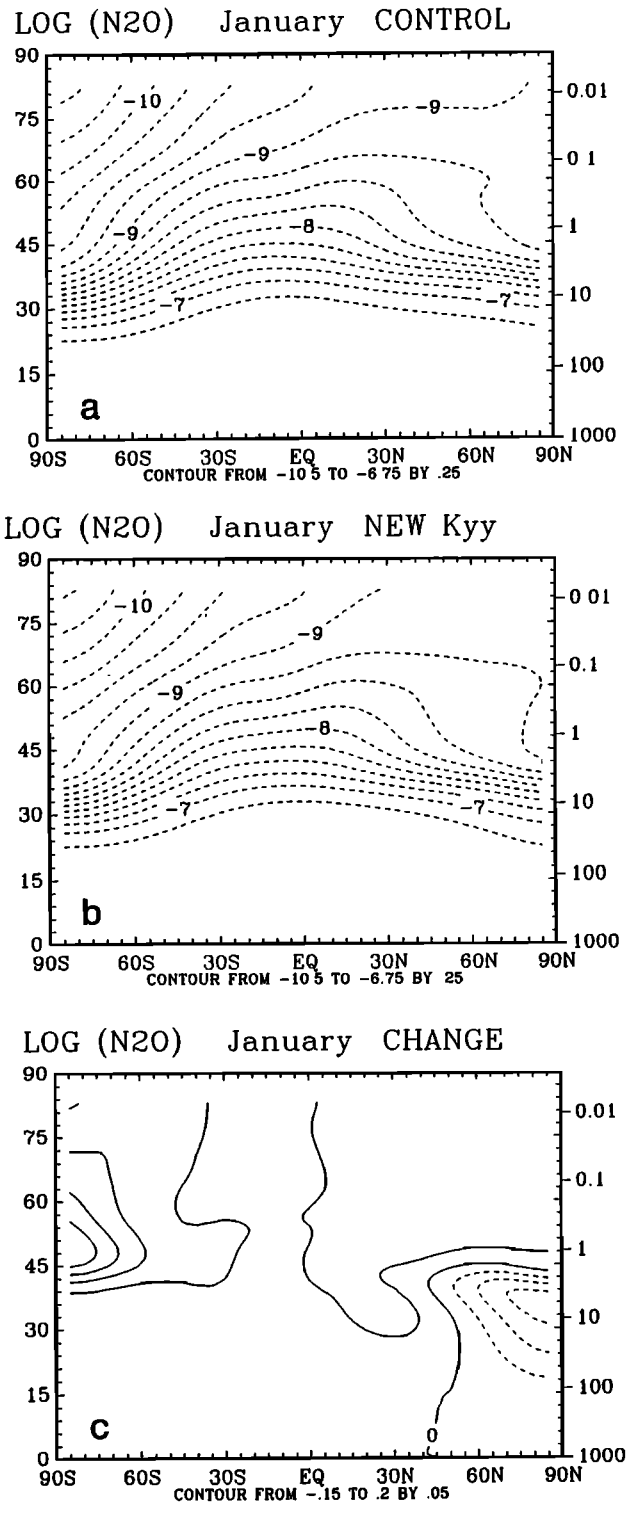

Fig. 15. As in Figure 13, but for $\log_{10}$ of N_2O mixing ratio.

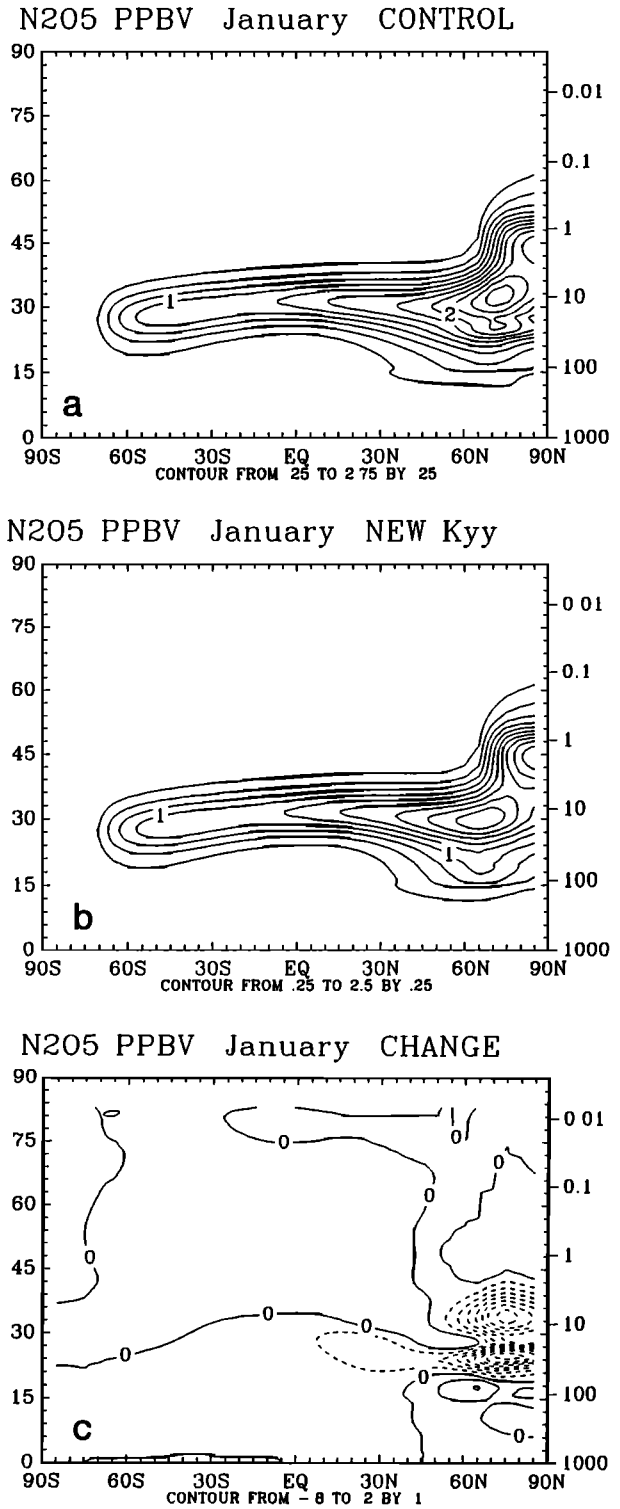

Fig. 16. As in Figure 13, but for N_2O_5 mixing ratio (ppbv).

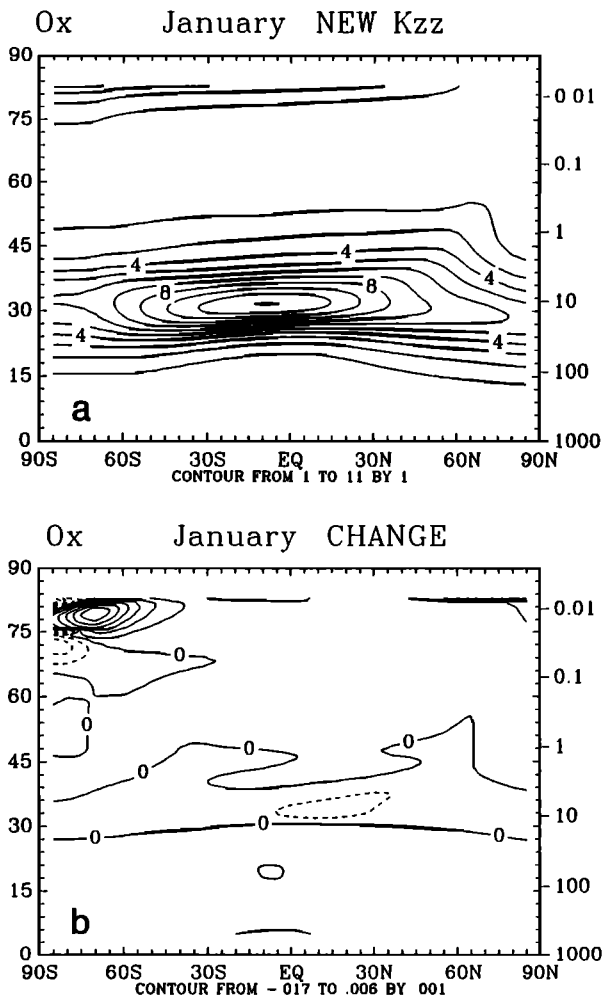

Fig. 17. Zonal mean O_x mixing ratio (ppmv) during January computed using (*a*) the control K_{yy} and chemical eddy K_{zz}; (*b*) Difference between the control (Figure 13*a*) and Figure 17*a*.

Figure 17*a* shows the odd oxygen distribution for a run with the chemical eddy parameterization used for vertical gravity wave transport, and with the control K_{yy}. Figure 17*b* shows the difference in O_x distribution between this run and the control case (Figure 13a). The differences are quite small everywhere, as expected from the similarities in the vertical transport coefficients (Figure 7 and 8).

6. Conclusions

Transport by waves is an important factor in controlling the distribution of trace species in the middle atmosphere. A crucial quantity for zonally averaged models is the net transport in the latitude height plane. Planetary Rossby waves reach large amplitudes in the stratosphere and lower mesosphere in the winter hemisphere and provide net transport that is primarily meridional. Gravity waves drive the mesospheric circulation and provide transport of heat and trace species there.

Since these waves cannot be explicitly modelled in a zonal average description, their effects are parameterized. The parameterizations used in our model are derived to determine the mean flow driving by the waves; the transport coefficients are then determined from these. This paper addresses the dependence of the transport coefficients on photochemical lifetime.

The wave transport is parameterized as independent meridional and vertical coefficients that require the assumption that eddy transport can be represented by the flux-gradient relation. The assumptions made in the derivation have three parts: (1) that all except meridional transport (K_{yy}) for Rossby waves and vertical transport (K_{zz}) for gravity waves can be

neglected, (2) that K_{yy} and K_{zz} are adequately represented by simple parameterizations based on zonal averaged fields and a specified boundary forcing, and (3) that the variations in K due to photochemistry derived using the linearized wave equation are adequate.

There is a strong theoretical basis for believing that the effective eddy transport coefficient (eddy flux divided by zonal mean gradient) varies substantially among species for those with a transition region, where dynamical and photochemical time scales are comparable. This paper describes a method of incorporating the chemical eddy contribution to parameterized transport in a 2D model and investigates its effect on the distribution of trace species. The conclusions are mixed. The chemical eddy contribution to Rossby wave transport has a significant impact; some of this is directly attributable to changes in the eddy transport and some to interdependence of the various chemical families in the model. For many species the chemical eddy parameterization gives very weak transport in the lower stratosphere, where the chemical lifetimes of most transported model constituents are long, resulting in steeper meridional gradients. For example, odd oxygen concentration is reduced in the high latitude lower stratosphere and comes somewhat closer to the observed distribution with the chemical eddy parameterization. N_2O_5 concentration is also less there than in the run without the chemical eddy effect included, but the reduction appears to result primarily from the reduction in production rate due to changes in the mixing ratio of ozone. The general conclusion is that the model changes are modest but significant with the Rossby wave parameterization altered to include the chemical eddy effect. On the other hand, the addition of the chemical eddy effect to the parameterized gravity wave transport has a negligible effect on the simulated distributions. It is not worth the additional model expense.

Various tests, in addition to those described in this paper, have been performed on the 2D model used in this study. These enable us to assess the impact of the chemical eddy modification to the transport matrix relative to other model changes. Even for those constituents on which it has the greatest impact, the change due to the chemical eddy transport is modest compared with that due to certain other modifications, particularly of those processes that drive the mean circulation. In particular the model climatology is sensitive to (1) substantial changes in the lower boundary (tropopause) stream function; (2) the employment of the complete radiative transfer calculation as opposed to a Newtonian cooling approximation, and (3) the implementation of the interactive Rossby wave parameterization to replace specified wave drag.

Acknowledgments. P. Newman made many helpful comments on an earlier version of this paper. Support for this work was provided by NSF grant ATM-8808562. Computing resources were provided by the Scientific Computing Division of National Center for Atmospheric Research (NCAR). NCAR is sponsored by the National Science Foundation.

REFERENCES

Andrews, D. G., and M. E. McIntyre, Planetary waves in horizontal and vertical shear: The generalized Eliassen-Palm relation and the mean zonal acceleration, *J. Atmos. Sci.*, *33*, 2031–2084, 1976.

Austin, J., R. R. Garcia, J. M. Russell III, S. Solomon, and A. F. Tuck, On the atmospheric photochemistry of nitric acid, *J. Geophys. Res.*, *91*, 5477–5485, 1986.

Brasseur, G., and M. Hitchman, The effect of breaking gravity waves on the distribution of trace species in the middle atmosphere, in *Transport Processes in the Middle Atmosphere*, edited by G. Visconti and R. Garcia, D. Reidel, Hingham, Mass., 1987.

Brasseur, G., M. H. Hitchman, S. Walters, M. Dymek, E. Falise, and M. Pirre, An interactive chemical dynamical radiative two-dimensional model of the middle atmosphere, *J. Geophys. Res.*, *95*, 5639–5655, 1990.

Chao, W. C., and M. R. Schoeberl, On the linear approximation of gravity wave saturation in the mesosphere, *J. Atmos. Sci.*, *41*, 1893–1898, 1984.

Charney, J. G. and P. G. Drazin, Propagation of planetary-scale disturbances from the lower into the upper atmosphere, *J. Geophys. Res.*, *66*, 83–109, 1961.

Coy, L., and D. C. Fritts, Gravity wave heat fluxes: A Lagrangian approach, *J. Atmos. Sci.*, *45*, 1770–1780, 1988.

Dunkerton, T. J. and D. P. Delisi, The subtropical mesospheric jet observed by the Nimbus 7 Limb Infrared Monitor of the Stratosphere. *J. Geophys. Res.*, *90*, 10,681–10,692, 1985.

Edmon, H. J., B. J. Hoskins and M. E., McIntyre, Eliassen-Palm cross sections for the troposphere, *J. Atmos. Sci.*, *37*, 2600–2616, 1980.

Evans, W. F. J., C. T. McElroy, and I. E. Galbally, The conversion of N_2O_5 to HNO_3 at high latitudes in winter, *Geophys. Res. Lett.*, *12*, 825–828, 1985.

Fritts, D. C., and T. J. Dunkerton, Fluxes of heat and constituents due to convectively unstable gravity waves, *J. Atmos. Sci.*, *42*, 549–556, 1985.

Garcia, R. R., and S. Solomon, A numerical model of the zonally averaged dynamical and chemical structure of the middle atmosphere, *J. Geophys. Res.*, *88*, 1379–1400, 1983.

Garcia, R. R., and S. Solomon, The effect of breaking gravity waves on the dynamics and chemical composition of the mesosphere and lower thermosphere, *J. Geophys. Res.*, *90*, 3850–3868, 1985.

Gille, J. C., Distributions of ozone and nitric acid measured by the Limb Infrared Monitor of the Stratosphere (LIMS), in *Transport Processes in the Middle Atmosphere*, edited by G. Visconti and R. Garcia, 73–85, D. Reidel, Hingham, Mass., 1987.

Gille, J. C., and L. V. Lyjak, Radiative heating and cooling rates in the middle atmosphere, *J. Atmos. Sci.*, *43*, 2215–2229, 1986.

Grose, W. L., J. E. Nealy, R. E. Turner, and W. T. Blackshear, Modeling the transport of chemically active constituents in the stratosphere, in *Transport Processes in the Middle Atmosphere*, edited by G. Visconti and R. Garcia, D. Reidel, Hingham, Mass., 1987.

Guthrie, P. D., C. H. Jackman, J. R. Herman, and C. J. McQuillan, A diabatic circulation experiment in a two-dimensional photochemical model, *J. Geophys. Res.*, *89*, 9589–9602, 1984.

Hartmann, D. L., and R. R. Garcia, A mechanistic model of ozone transport by planetary waves in the stratosphere, *J. Atmos. Sci.*, *36*, 350–364, 1979.

Hitchman, M. H., and G. Brasseur, Rossby wave activity in a 2-D model: Closure for wave driving and meridional eddy diffusivity, *J. Geophys. Res.*, *93*, 9405–9417, 1988.

Holton, J. R., An advective model for two-dimensional transport of stratospheric trace species, *J. Geophys. Res.*, *86*, 11,989–11,994, 1981.

Holton, J. R., and M. R. Schoeberl, The role of gravity wave generated advection and diffusion in transport of tracers in the mesosphere, *J. Geophys. Res.*, *93*, 11,075–11,082, 1988.

Hoskins, B., J. McIntyre, and A. W. Robertson, On the use and significance of isentropic potential-vorticity maps, *Q. J. R. Meteorol. Soc.*, *111*, 877-946, 1985.

Jones, R. L., and J. A. Pyle, Observations of CH_4 and N_2O by the Nimbus 7 SAMS: A comparison with in situ data and two-dimensional numerical model calculations, *J. Geophys. Res.*, *89*, 5263–5279, 1984.

Kaye, J. A., and R. B. Rood, Chemistry and transport in a three-dimensional stratospheric model: Chlorine species during a simulated stratospheric warming, *J. Geophys. Res.*, *94*, 1057–1083, 1989.

Ko, M. K. W., K. K. Tung, D. K. Weisenstein, and N. D. Sze, A zonal mean model of stratospheric tracer transport in isentropic coordinates: Numerical simulations for nitrous oxide and nitric acid, *J. Geophys. Res.*, *90*, 2313–2329, 1985.

Lindzen, R. S., Turbulence and stress owing to gravity wave and tidal breakdown. *J. Geophys. Res.*, *86*, 9707–9714, 1981.

Mahlman, J. D., and W. J. Moxim, Tracer simulation using a global

general circulation model: Results from midlatitude instantaneous source experiment, *J. Atmos. Sci., 35*, 1340–1374, 1978.

Mahlman, J. D., and L. J. Umscheid, Comprehensive modeling of the middle atmosphere: The influence of horizontal resolution, in *Transport Processes in the Middle Atmosphere*, edited by G. Visconti and R. Garcia, D. Reidel, Hingham, Mass., 1987.

Matsuno, T., Lagrangian motion of air parcels in the stratosphere in the presence of planetary waves, *Pure Appl. Geophys., 118*, 189–216, 1980.

McIntyre, M. E., and T. N. Palmer, Breaking planetary waves in the stratosphere, *Nature, 305*, 593–600, 1983.

McPeters, R. D., D. F. Heath and P. K. Bhartia, Average ozone profiles for 1979 for the Nimbus 7 SBUV instrument, *J. Geophys. Res., 89*, 5199–5214, 1984.

Newman, P. A., M. R. Schoeberl, and R. A. Plumb, Horizontal mixing coefficients for two-dimensional chemical models calculated from National Meteorological Society data, *J. Geophys. Res., 91*, 7919–7924, 1986.

Newman, P. A., M. R. Schoeberl, R. A. Plumb, and J. E. Rosenfeld, Mixing rates calculated from potential vorticity, *J. Geophys. Res., 93*, 5221–5240, 1988.

Pitari, G., and G. Visconti, Two-dimensional tracer transport: Derivation of residual mean circulation and eddy transport tensor from a 3-D model data set, *J. Geophys. Res., 90*, 8019–8032, 1985.

Plumb, R. A., Eddy fluxes of conserved quantities by small-amplitude waves, *J. Atmos. Sci., 36*, 1699–1704, 1979.

Plumb, R. A., and J. D. Mahlman, The zonally averaged transport circulation characteristics of the GFDL general circulation / transport model, *J. Atmos. Sci., 44*, 298–327, 1987.

Pyle, J. A., and C. F. Rogers, Stratospheric transport by stationary planetary waves—The importance of chemical processes, *Q. J. R. Meteorol. Soc., 106*, 421–446, 1980.

Rose, K., and G. Brasseur, A three-dimensional model of chemically active trace species in the middle atmosphere during disturbed winter conditions, *J. Geophys. Res., 94*, 16,387–16,403, 1989.

Schneider, H. R., M. K. W. Ko, N. D. Sze, G.-Y. Shi, and W.-C. Wang, An evaluation of the role of eddy diffusion in stratospheric interactive two-dimensional models, *J. Atmos. Sci., 46*, 2079–2093, 1989.

Schoeberl, M. R. and A. K. Smith, The integrated enstrophy budget of the winter stratosphere diagnosed from LIMS data, *J. Atmos. Sci., 43*, 1074–1086, 1986.

Schoeberl, M. R., A model of gravity wave breakdown with convective adjustment, *J. Atmos. Sci., 45*, 980–992, 1988.

Schoeberl, M. R., D. F. Strobel, and J. Apruzese, A numerical model of gravity wave breaking and stress in the mesosphere, *J. Geophys. Res., 88*, 5249–5259, 1983.

Smith, A. K., L. V. Lyjak, and J. C. Gille, The eddy transport of nonconserved trace species derived from satellite data, *J. Geophys. Res., 93*, 11,103–11,122, 1988.

Stordal, F., I. S. A. Isaksen and K. Horntveth, A diabatic circulation two-dimensional model with photochemistry: Simulations of ozone and long-lived tracers with surface sources, *J. Geophys. Res., 90*, 5757–5776, 1985.

Strobel, D. F., Parameterization of linear wave chemical transport in planetary atmospheres by eddy diffusion, *J. Geophys. Res., 86*, 9806–9810, 1981.

Strobel, D. F., J. P. Apruzese, and M. R. Schoeberl, Energy balance constraints on gravity wave induced eddy diffusion in the mesosphere and lower thermosphere. *J. Geophys. Res., 90*, 13,067–13,072, 1985.

Strobel, D. F., M. E. Summers, R. M. Bevilacqua, M. T. DeLand, and M. Allen, Vertical constituent transport in the mesosphere, *J. Geophys. Res., 92*, 6691–6698, 1987.

Tung, K. K., On the two-dimensional transport of stratospheric trace gases in isentropic coordinates. *J. Atmos. Sci., 39*, 2330–2355, 1982.

Tung, K. K., A coupled model of zonally averaged dynamics, radiation and chemistry, in *Transport Processes in the Middle Atmosphere*, edited by G. Visconti and R. Garcia, D. Reidel, Hingham, Mass., 1987.

Wehrbein, W. M., and C. B. Leovy, An accurate radiative heating and cooling algorithm for use in a dynamical model of the middle atmosphere, *J. Atmos. Sci., 39*, 1532–1544, 1982.

G. P. Brasseur, National Center for Atmospheric Research, P. O. Box 3000, Boulder, CO 80307.

A. K. Smith, Space Physics Research Laboratory, Department of Atmospheric, Oceanic and Space Science, University of Michigan, Ann Arbor, MI 48109.

(Received October 23, 1989;
revised February 14, 1990;
accepted February 14, 1990.)